Electronic Supplementary Information

Complex formation of silver(I) ion with a glucosinolate derivative: structural and mechanistic insights into myrosinase-mimicking C-S bond cleavage

Laurenzo Alba, Tsubasa Hatanaka, Francisco Franco Jr., Masaki Nojiri, Marissa Noel and Yasuhiro Funahashi

References

1. Experimental section

1.1. Materials and Measurements

All experiments were carried out in air. (-)-sinigrin hydrate, silver triflate, pyridine, acetic anhydride, and methanol were used as supplied and without further purification. All the reagents were of analytical grade or highest grade available. (-)-sinigrin hydrate and silver triflate were purchased from Aldrich.

^{1}H NMR spectra were recorded with a JEOL ECS400 at 400 MHZ. Solvents used in NMR experiments were DMSO-d_6 or MeOH-d_4 depending on sample solubility. ^{1}H NMR spectra were referenced to the residual proton peak of the deuterated solvent. Elemental analyses were carried out with a Yanaco CHN Corder MT-6 analyzer. The details in collection of X-ray diffraction data and calculation for structural refinements are described in the following **1.5** and cif files.

1.2. Synthesis

1.2.1. Synthesis of tetra-O-acetyl sinigrin potassium salt (K·SinAc)

It is noted that the synthesis of Sin-Ac was previously described by Schultz and Wagner (1955)[1]. The following method uses different reagent proportions and recrystallization solvent for a smaller scale. Sinigrin (50.48 mg) was weighed into a 10-mL round-bottomed flask with a stirring bar. It was suspended in 389 μL of pyridine and stirred over an ice bath. Acetic anhydride (107 μL) was slowly added while stirring. The stirring was continued for 30 minutes over ice, then the ice was replaced with a room-temperature water bath. Stirring was continued for 2 hours. During this time, the suspension became a clear solution, which eventually transformed into a colorless gel-like substance during the final 30 minutes. The mixture was then evaporated completely using a vacuum line with cold trap, resulting in a white powder. This powder was dissolved in about 25 mL methanol to form a clear solution, which was placed in an open vial and allowed to evaporate overnight to about 15% of its original volume, resulting in the formation of crystalline product. The vial was then sealed and placed in the freezer to precipitate more crystals. The remaining methanol solution was removed by pipette, and the crystals are allowed to dry in air for 1 day. Yield: 47.5 mg (66.1%). ^{1}H-NMR (400 MHz, MeOH-d_4) δ 6.05 (ddt, J = 6 Hz, 10.4 Hz, 17.6 Hz, 1H), 5.35 (d, J = 10 Hz, 1H), 5.34 (t, J = 9.4 Hz, 1H), 5.30 (dq, J = 1.6 Hz, 17.6 Hz, 1H), 5.21 (dq, J = 1.6 Hz, 10.4 Hz, 1H), 5.04 (t, J = 9.8 Hz, 1H), 4.98 (dd, J = 9.2 Hz, 10 Hz, 1H), 4.23 (dd, J = 5.6 Hz, 12.8 Hz, 1H), 4.16 (dd, J = 2.4 Hz, 12.8 Hz, 1H), 3.98 (ddd, J = 2.4 Hz, 5.6 Hz, 10.4 Hz, 1H), 3.47 (dt, J = 1.6 Hz, 6 Hz, 2H), 2.06 (s, 3H), 2.02 (s, 6H), 1.96 (s, 3H). Anal. Calcd. for $C_{18}H_{24}NO_{13}S_2K$: C 38.23; H 4.28; N 2.48%; Found C 38.06; H 4.33; N 2.62%.

1.2.2 Synthesis of silver tetra-O-acetyl sinigrin complex (Ag·SinAc)

In a 10-mL screw-capped vial, acetylated sinigrin (14.1 mg, 1 eq.) was dissolved in a minimum amount of methanol. To it was added a solution containing 11.2 mg silver triflate (1.75 eq.) in methanol and swirled for 15 minutes, resulting in a clear, colorless solution. The solution was very carefully evaporated by light application of vacuum until white or colorless needle crystals start to appear. Upon the appearance of the first crystals, the vial was then capped and placed in the refrigerator for 3 days. The crystals were collected by decantation, washed with ether, and rapidly air-dried for analysis. Yield: 13.0 mg (82.2%) 1H-NMR (400 MHz, MeOH-d_4) δ 6.19 (ddt, J = 6.4 Hz, 10 Hz, 17.6 Hz, 1H), 5.45-5.36 (m, 2H), 5.42 (d, J = 10 Hz, 1H), 5.36 (t, J = 9.2 Hz, 1H), 5.06 (t, J = 9.2 Hz, 1H), 5.03 (t, J = 9.2 Hz, 1H), 4.20 (d, J = 4.4 Hz, 2H), 4.02 (dt, J = 4 Hz, 10.4 Hz, 1H), 3.59 (dd, J = 1.2 Hz, 6.4 Hz, 2H), 2.06 (s, 3H), 2.04 (s, 3H), 2.03 (s, 3H),

1.98 (s, 3H). Anal. Calcd. for $C_{18}H_{24}NO_{13}S_2Ag$: C 34.08; H 3.81; N 2.21%; Found C 33.86; H 3.87; N 2.22%. The product is air-stable but slowly decomposes upon prolonged exposure to light, forming a black residue.

1.3 Solution equilibrium of Ag^+-$SinAc^-$ complexation

^{1}H NMR spectra changed with the addition of AgOTf to **K·SinAc**$^-$ in MeOH-d_6 solution. Based on the saturation behavior of the chemical shift changes in the vinylic and anomeric protons, we evaluated the equilibrium reaction of Ag^+-**SinAc**$^-$ complexation as follows (M = Ag^+, L = **SinAc**$^-$, δ_x = chemical shift values, C_x = total concentrations).

$C_M = xC_L$ (x eq.)

$$log\frac{\delta_{obs.} - \delta_L}{\delta_{ML} - \delta_{obs.}} = n \cdot log\left(x - \frac{\delta_{obs.} - \delta_L}{\delta_{ML} - \delta_L}\right) + logK + n \cdot logC_L \qquad (1)$$

$n = 1$: M + L $\rightleftarrows$ ML $\qquad K = \frac{[ML]}{[M][L]}$

$n = 2$: 2M + L $\rightleftarrows$ M_2L $\qquad K = \frac{[M_2L]}{[M]^2[L]}$

The preliminary analysis using equation (1) gave n = 0.95, indicating that a 1:1 ratio of Ag^+-**SinAc**$^-$ complexation is dominant. Then, we further estimated formation constant of the Ag^+-**SinAc**$^-$ complexation by using the following equation (2), and simulated fitting curves of the observed chemical shift plots. The estimated value on chemical shift changes of the internal vinylic proton H15 are shown in the main text.

$$\delta_{obs.} = \delta_L + (\delta_{ML} - \delta_L) \cdot \frac{K \cdot C_M}{1 + K \cdot C_M} \qquad (2)$$

1.4 Thermal decomposition of Ag·SinAc

K·SinAc (1 eq.) in methanol was mixed with a solution of AgOTf (2 eq.) in methanol. Partial evaporation of this solution at room temperature produced crystals of **Ag·SinAc** *in situ*. This solution was then heated to about 50° C, causing the redissolution of all crystalline precipitates previously formed. A new white powder precipitate was generated in 15 min on standing at room temperature. This precipitate was isolated by centrifugation, washed with MeOH, dried, and dissolved in DMSO-d_6 for analysis.

1.5 X-ray crystallographic analysis of K·SinAc and Ag·SinAc

Single crystals were grown for **K·SinAc** and **Ag·SinAc** and mounted on nylon loops while immersed in mineral oil. Both were analyzed with a Rigaku XTALab Synergy-S diffractometer. X-ray diffraction data were acquired under a stream of liquid nitrogen vapor at 173K and using Mo-Kα radiation (λ = 0.71073 Å). The other details can be referred to the cif files.

Calculations were performed with the Olex2 software[2]. All structures were solved by direct methods[3] and the structure was expanded with Fourier techniques. Structural refinements were performed with ShelXL v. 2014/6 using Least Squares minimization.

For **K·SinAc**, all non-hydrogen atoms were refined anisotropically. Hydrogen atoms were placed at calculated positions using the riding model.

For **Ag·SinAc**, the maximum reflection range used to refine 2θmax was reduced from 55° to 52°. The C5, C6, O10, O11, C32, and O33 atoms were modelled as disordered over two positions with 67% and 33% occupancies; these atoms are refined isotropically. The EADP command was used to constrain the temperature factors of the minor part of the structure. Hydrogen atoms were placed at calculated positions using the riding model.

1.6. Computational study

Density functional theory (DFT) calculations were carried out with the Gaussian16 quantum chemistry package[4]. The starting structures of the complexes were taken from the X-ray crystal coordinates, and equilibrium structures were determined with the PBE0 functional and 6-31+G(d,p) basis set for all atoms, except for the metals, which were modeled using the LANL2DZ core potential basis set. To account for the non-covalent interactions due to dispersion forces, Grimme's dispersion correction with Becke-Johnson Damping (D3-BJ)[5,6] was also included and the solvent effect was considered using the self-consistent reaction field (SCRF) method based on the polarization continuum model (PCM)[7] with methanol as the solvent. Frequency calculations also at the same level (PBE0-D3(BJ)/6-31+G(d,p)-LANL2DZ) were then carried out to make sure that the structures correspond to true minima. The thermodynamic quantities were determined at 298.15 K and the heterolytic bond dissociation enthalpy (BDE_{het}) was obtained using equation (3):

$$BDE_{het} = H(\text{Ag+-thio}^-) + H(\text{glu}^+) - H(\text{Ag+-}\mathbf{SinAc}^-) \quad (3)$$

where H(Ag+-**SinAc**$^-$) is the enthalpy for the **SinAc**$^-$ complex, while H(Ag-thio$^-$) and H(glu$^+$) are the enthalpies of the heterolytically dissociated fragments. The NBO population analysis was carried out using the NBO program[8] and the molecular structures were viewed using Chemcraft[9].

2. **Supplementary Figures and Tables**

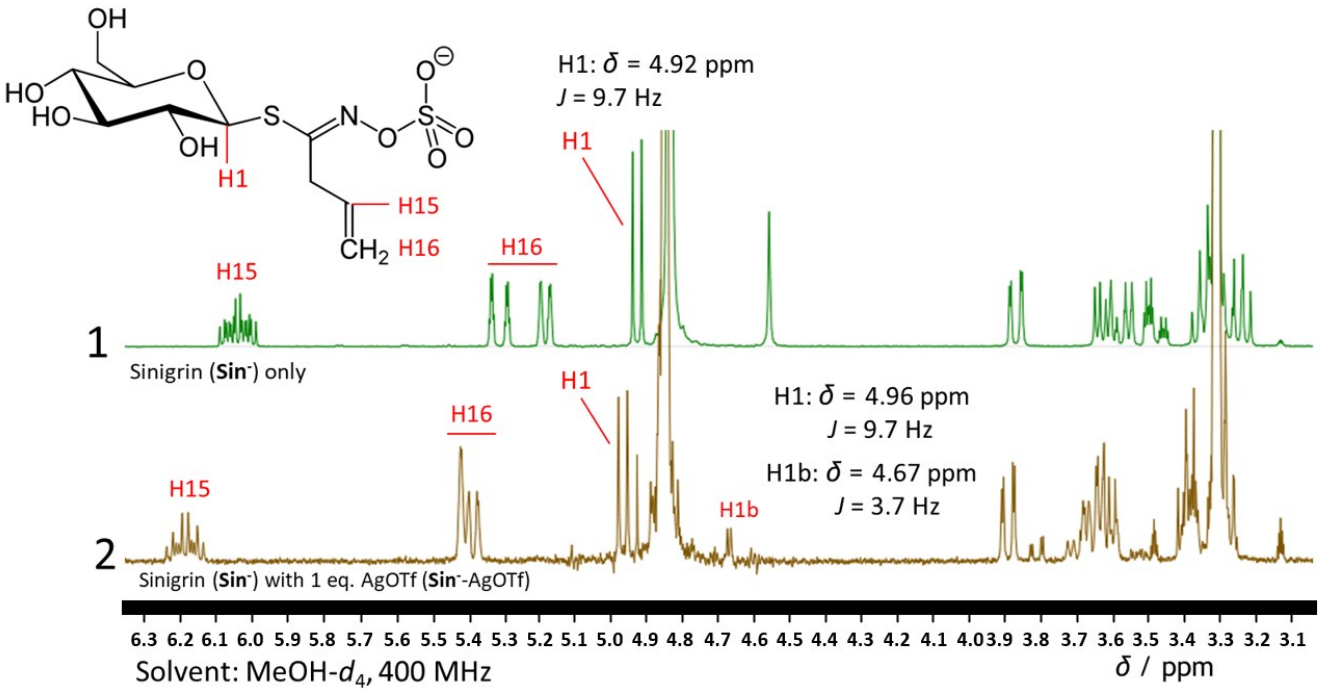

1. Sinigrin was dissolved in MeOH-d_4 (5 mM).
2. 1 eq. of AgOTf was added to 1.

* The axial H1 of Sin is changing to the equatorial H1b of product sugar in part.

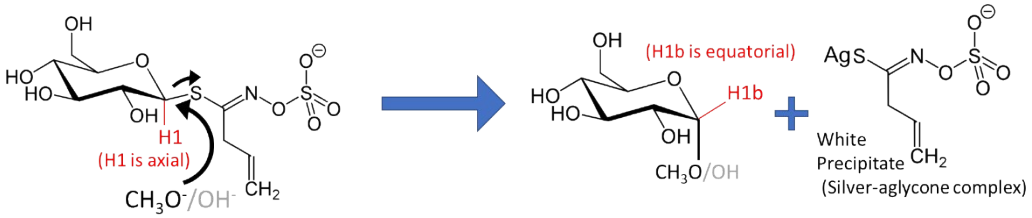

Fig. S1 ^{1}H NMR spectra of **1**. sinigrin (**Sin**$^-$) only before the addition of AgOTf and **2**. after addition of 1 eq. AgOTf to **1**. 400 MHz, in MeOH-d_4.

*^{1}H NMR spectral changes of vinylic protons of **Sin**$^-$ with the addition of AgOTf

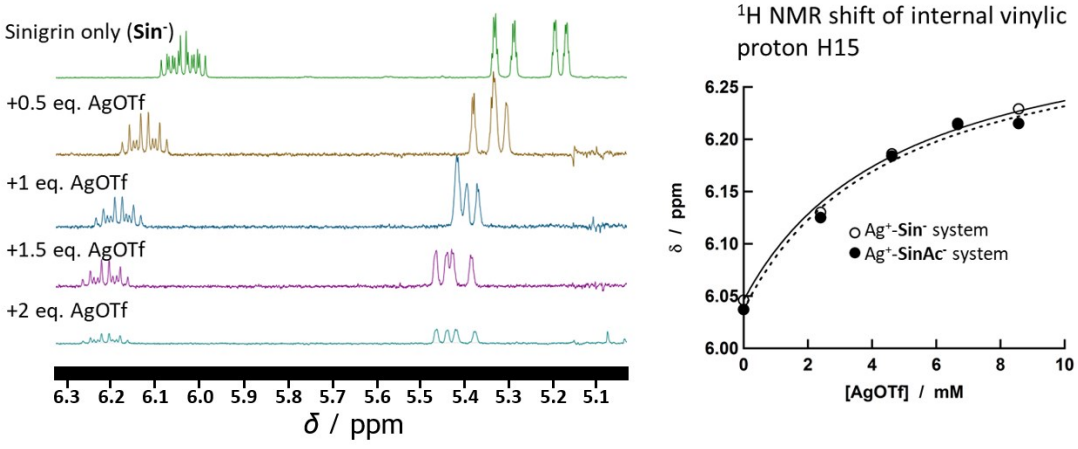

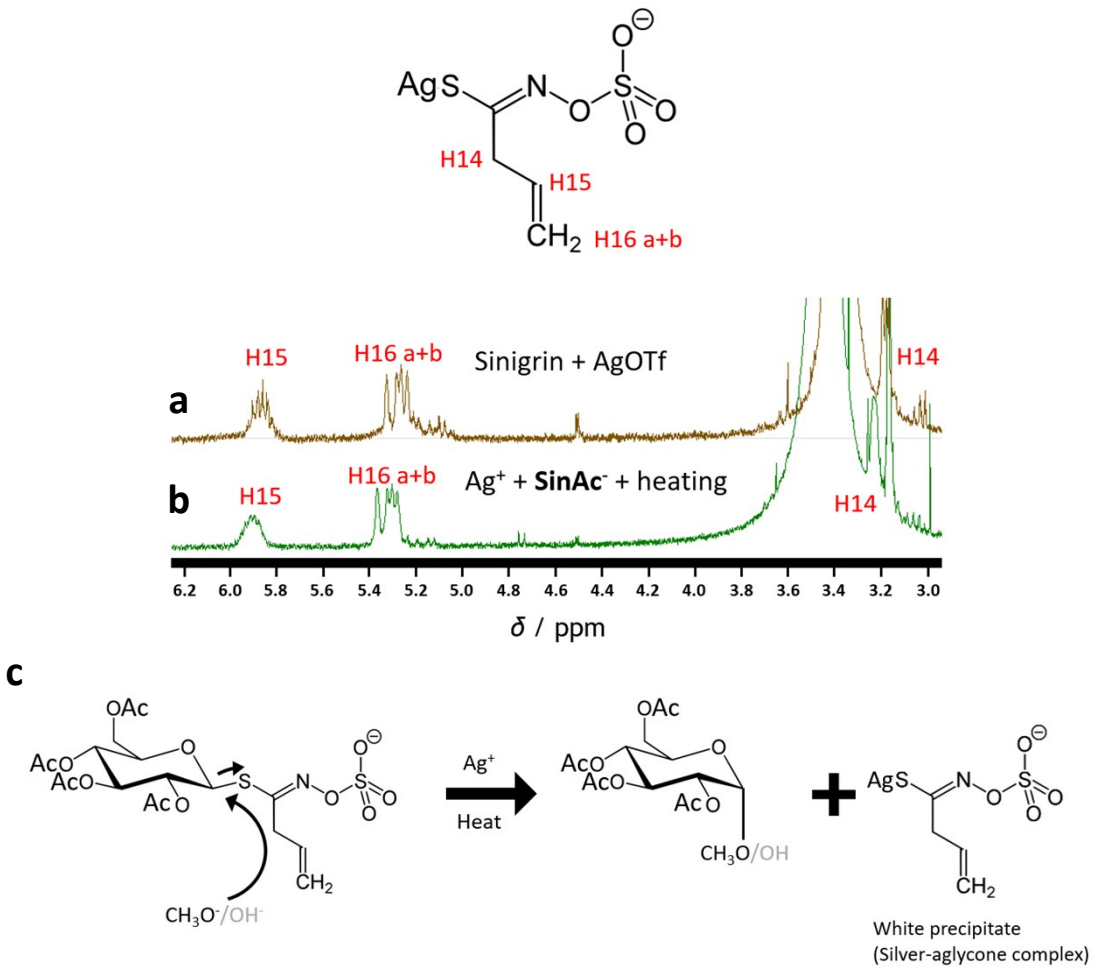

Fig. S2 ^{1}H NMR spectra of decomposition product of **Sin**$^{-}$ with silver (**a**), or Ag^{+}-**SinAc**$^{-}$ (**b**) in DMSO-d_6, measured at 400 MHz. Proton assignments are labeled according to the structure shown above. The silver-catalyzed breakage of the C-S bond of **SinAc**$^{-}$ in methanol is shown in (**c**).

Fig. S2 shows the ^{1}H NMR spectra of the precipitates isolated from the reaction of **Sin**$^{-}$ with silver(I) (Fig. S2a), or the reaction of **SinAc**$^{-}$ with silver (I) with the application of heat (Fig. S2b). Fig. S2c shows proposed reaction mechanism yielding the Ag-aglycone. The peaks in the spectra are within or close to the range of chemical shifts reported in an earlier study on potassium silver aglycone measured in D_2O (1-proton multiplet at 392-350 Hz (6.53-5.83 ppm), 2-proton signal at 337-313 Hz (5.61-5.21 ppm), 2-proton doublet at 201 Hz (3.35 ppm), 60 MHz spectrometer).[10] Additionally, these spectra of Ag-aglycone complex are distinct from that of allyl isothiocyanate measured in DMSO-d_6 (internal vinylic proton signals at 5.85-5.96 ppm, terminal vinylic proton signals at 5.23-5.35 ppm, and the methylene proton signals at 4.29-4.33 ppm). In contrast, the H14 methylene signals of the Ag-aglycone complex are observed at around 3.2 ppm. This feature is characteristic of the Ag-aglycone complex as previously reported (3.35 ppm).[10]

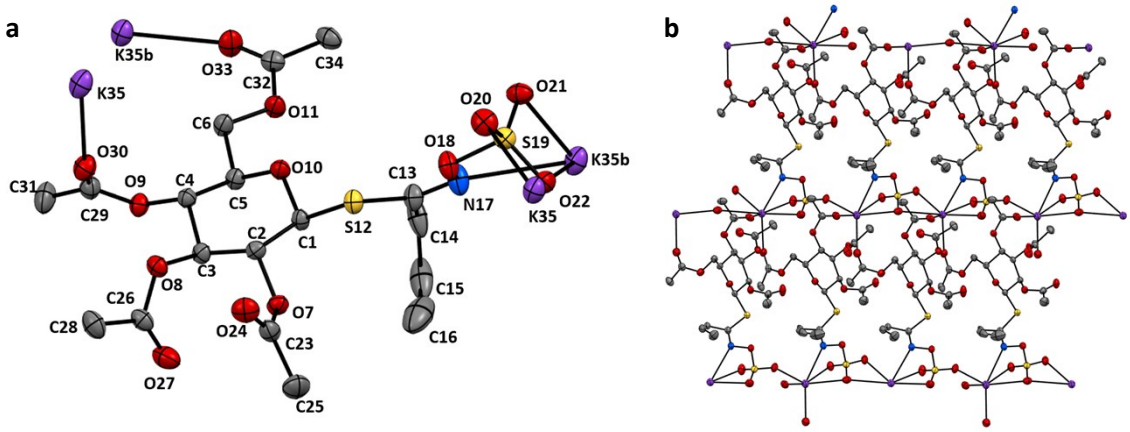

Fig. S3 **a.** (left) ORTEP view of part of the molecular structure of **K·SinAc** with atom numbering. **b.** (right) 2D sheet network of **SinAc**$^-$ with potassium ions. Hydrogens are omitted for clarity. Thermal ellipsoids are drawn at 50% probability level.

***** Structural description of **K·SinAc**

Sin$^-$ was acetylated using a modification from the method previously reported[1] and recrystallized from methanol. The synthesis of tetra-*O*-acetyl sinigrin potassium salt (**K·SinAc**), crystallographic data and selected bond distances are tabulated (Fig S3, Table S1, and Table S2). The ^{1}H NMR spectrum of **K·SinAc** in MeOH-d_4 confirms the chair conformation and equatorial arrangement of acetyl groups as well as the β conformation of the glycosidic bond in solution (Fig. S4), being consistent with those in the crystalline solid state.

Fig. S3a shows the structure of one molecule of **SinAc**$^-$ in the solid state with atom numbering. An asymmetric unit is free of disorder or solvent molecules and contains two molecules of **SinAc**$^-$ linked by potassium ions to form a polymeric lattice. The sugar moiety adopts a standard chair conformation with all the acetyl groups and the glycosidic allyl portion in equatorial positions. The bond distances and angles within the sugar ring and acetyl groups are typical for an acetylated monosaccharide.[11] The bond length between C1 and S12 is 1.800 or 1.802 Å, and from S12 to C13 is either 1.747 or 1.761 Å, with an angle of 104.56 or 101.96°, the bond distances and angles of one of the **SinAc**$^-$ molecules are very similar to those of the potassium salt of sinigrin (**Sin**$^-$)[12] while the other **SinAc**$^-$ molecule has a slightly different set of bond distances and angles.

The K^+ ions occur in two distinct positions in the asymmetric unit and are either six- or seven-coordinated. K ions are coordinated to distinct sulfate oxygens by three or four bonds ranging from 2.606 to 3.108 Å, the latter of which is longer than the sum of the van der Waals radii of both atoms. The lengths of these bonds are comparable the range of distances found in **Sin**$^-$.[12] Unlike **Sin**$^-$, however, the K^+ ions are also singly coordinated to the N atom with a distance of 2.943-2.987 Å. Additionally, each K^+ ion is coordinated to two neighboring carbonyl O atoms of the acetyl groups from separate **SinAc**$^-$ molecules.

The **SinAc**$^-$ molecules are arranged in two-dimensional sheets with the plane of the sugar ring oriented diagonally and rotated in the same direction as the others. K^+ ions form the intermolecular links within the sheet only. The hydrocarbon portion of the allyl moiety projects into a pocket between two neighboring sugars in a sheet (Fig. S3b).

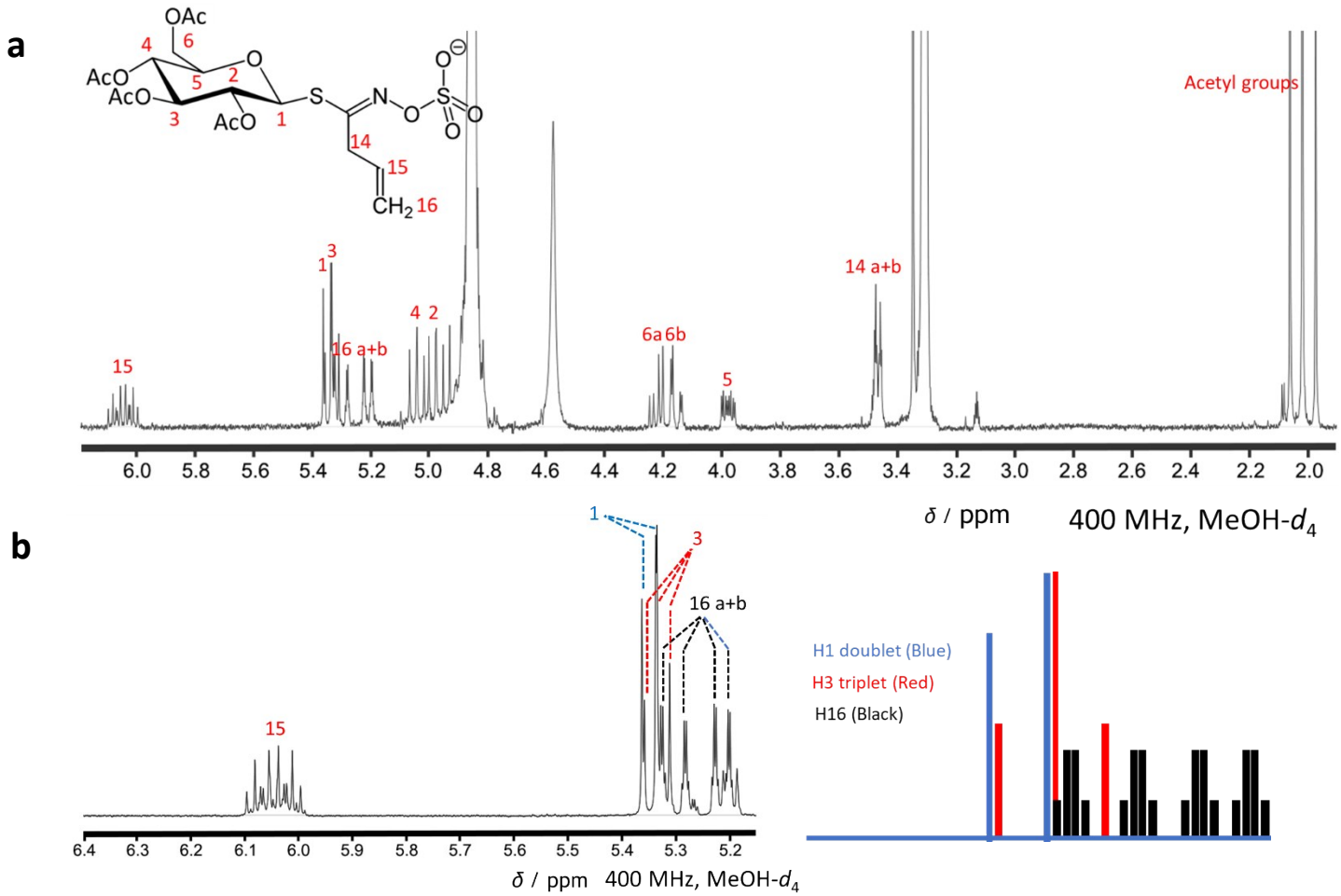

1) Chemical shifts of two H signals of the terminal vinylic protons are different.
2) The H signal of one terminal vinylic proton is split by coupling with the other vinylic proton (doublet). The two signals of terminal vinylic protons are in four.
3) The one signal of vinylic proton is split in two (doublet) by coupling with the internal vinylic proton. It is further split in two (doublet) by strongly coupling with one of the two methylene protons, depending on their torsion angles.

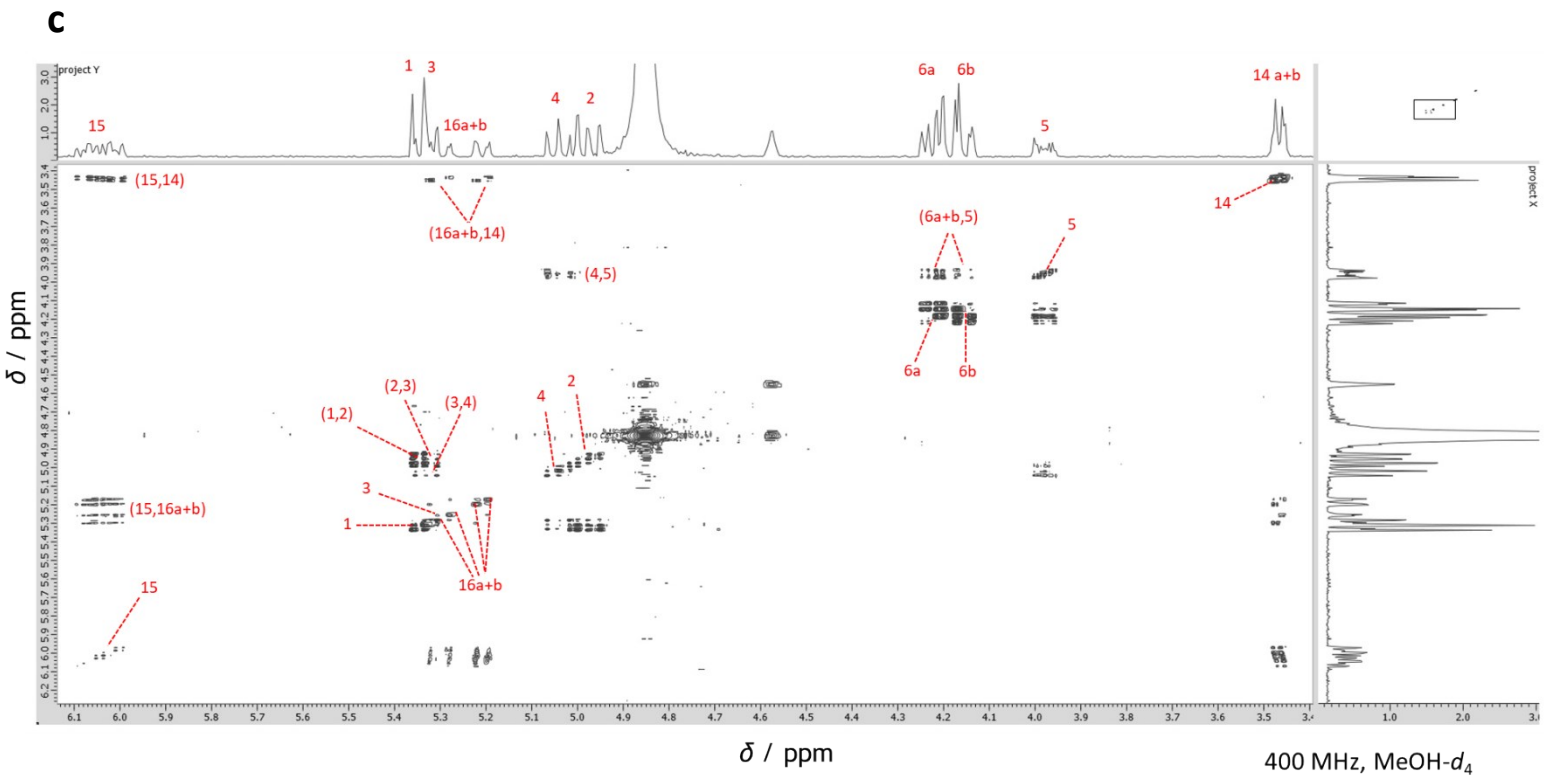

Fig. S4 **a.** ^{1}H NMR spectrum of **K·SinAc** in MeOH-d_4. **b.** Details on the assignment of **K·SinAc** in the ^{1}H NMR peaks above 5.2 ppm. **c.** ^{1}H-^{1}H COSY spectra of **K·SinAc**. Acetyl group protons (found ca. 2 ppm) are excluded.

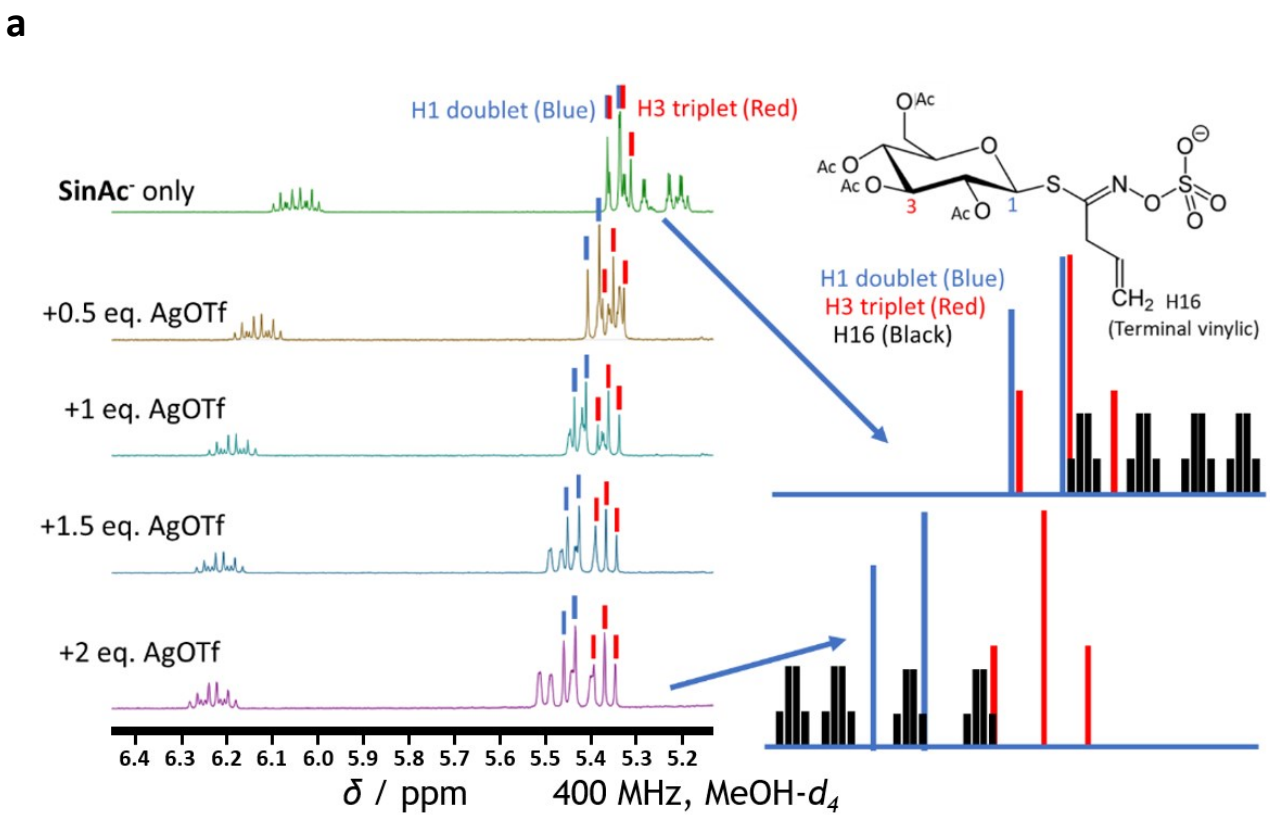

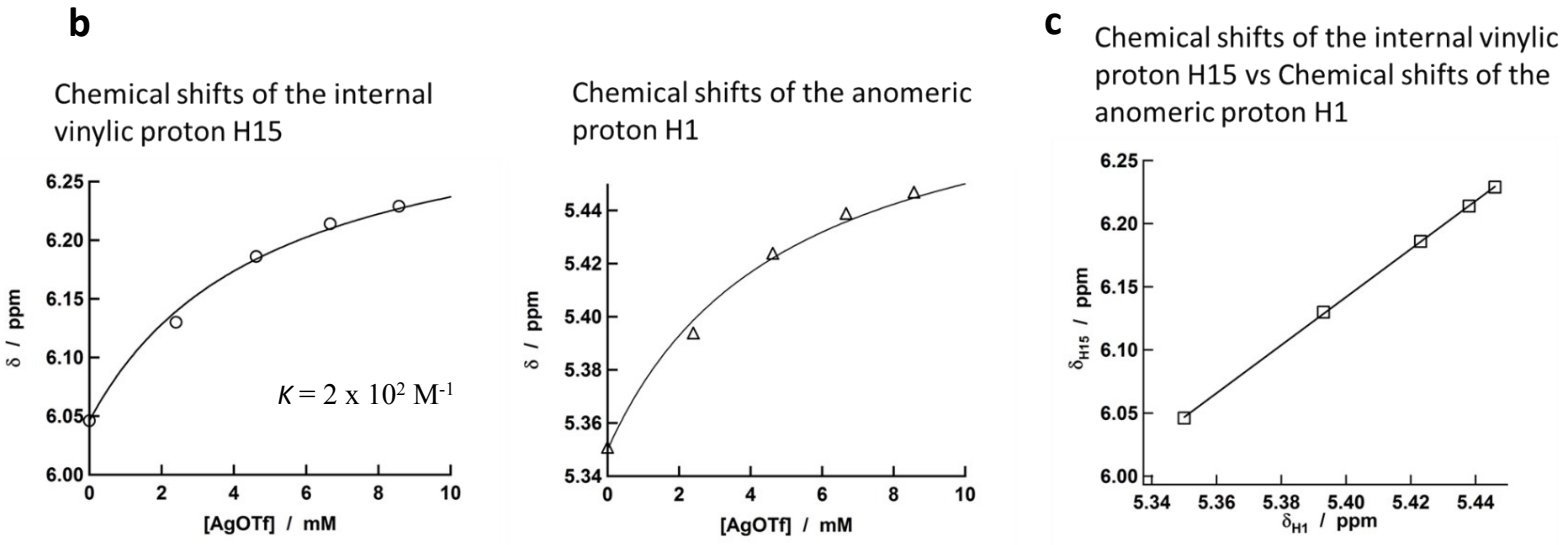

Fig. S5 **a.** Details of ^{1}H NMR spectral changes of anomeric H1 and vinylic protons H15, H16 of **SinAc**$^{-}$ with the addition of AgOTf. **b.** Plots of chemical shifts of the anomeric H1 and internal vinylic H15 vs [AgOTf]. **c.** Plots of chemical shifts of H1 vs chemical shifts of H15 in the Ag^{+}-**SinAc**$^{-}$ systems. 400 MHz, in MeOH-d_4.

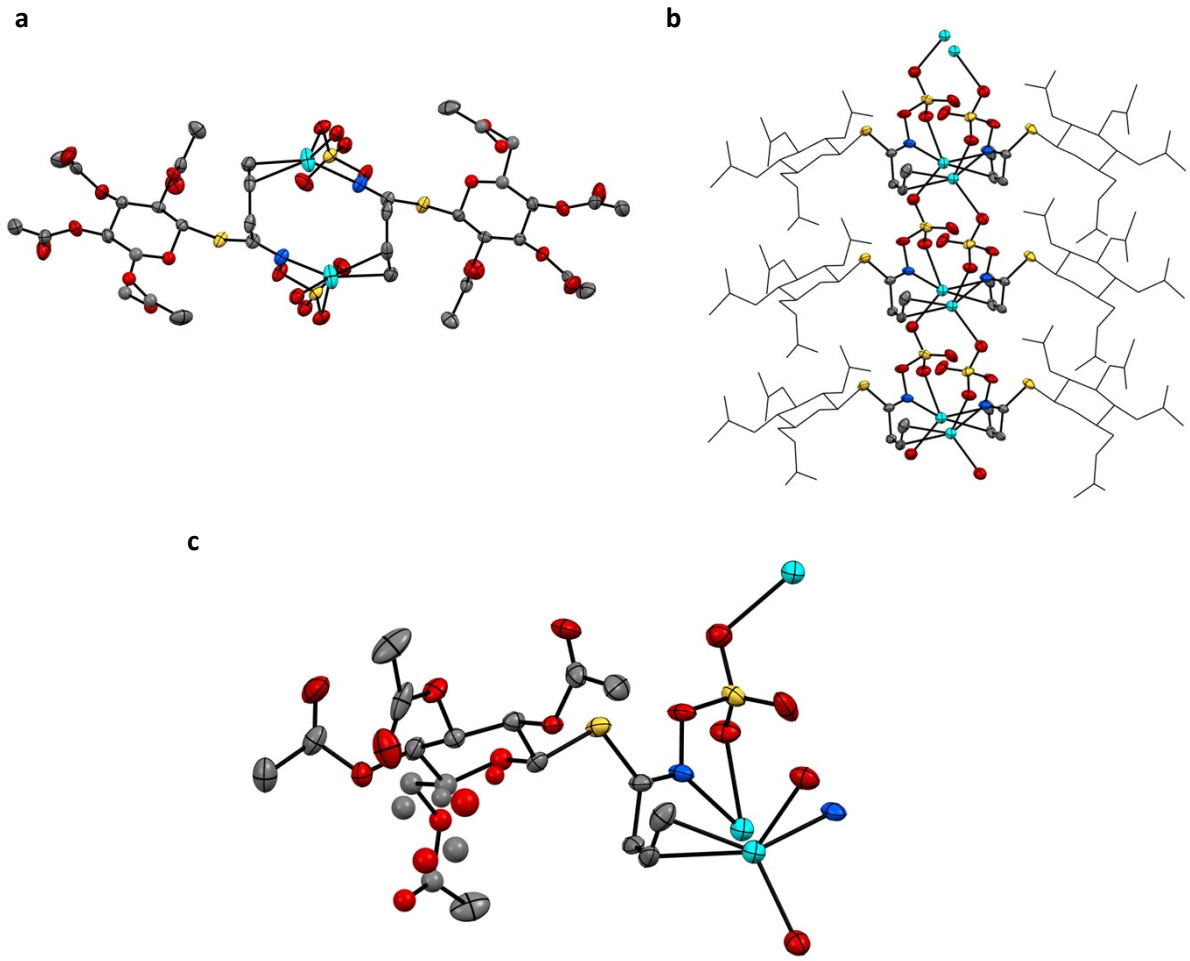

Fig. S6 **a.** (left) Pair of **Ag·SinAc** showing central ring structure. **b.** (right) 1D chain structure of **Ag·SinAc**. **c.** (bottom) The structure with the disordered atoms. Hydrogens are omitted for clarity. Thermal ellipsoids are drawn at 50% probability level.

* Additional structural details of **Ag·SinAc**

The C5, C6, O10, O11, C32, and C33 atoms are disordered across two positions; interestingly, this disorder is also reflected in the ^{1}H NMR spectrum of **Ag·SinAc** in solution through the merging of the two signals of the diastereotopic protons attached to C6.

The **Ag·SinAc** molecules can be thought of as arranged in pairs (Fig. S6a), with a central ring composed of two silver ions coordinated to two allyl groups, and the remaining site of each silver ion is coordinated to sulfates belonging to the next pair of Ag^{+}-**SinAc**$^{-}$ molecules.

The molecules of Ag^{+}-**SinAc**$^{-}$ are organized into chains with the sugar moieties projecting on either side (Fig. S6b), with a central core composed of the silver ions and the coordinated allyl groups.

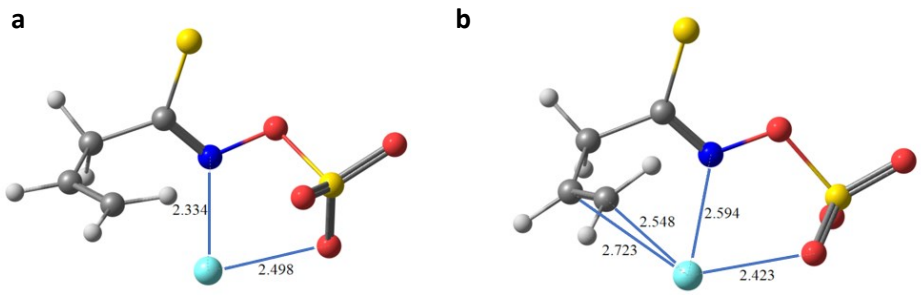

Fig. S7 Calculated structures of Ag^+-aglycone complex based on the two most stable conformations of the intact Ag^+-**SinAc**$^-$ complex. Structure **a** (left) is based on **3a**, while **b** (right) is based on **3b**.

Structural simulations were carried out for the Ag-aglycone complexes based on the DFT-optimized structures **3a** and **3b**, respectively. The structure **b** has lower energy by 2.6 kJ/mol than **a** due to the chelate ring effect, and thus more likely represents the product structure. The complexation with Ag^+ stabilizes this leaving group further and therefore accelerates the hydrolysis of sinigrin. Further crystallographic studies on the silver-aglycone complex are needed to confirm these structures.

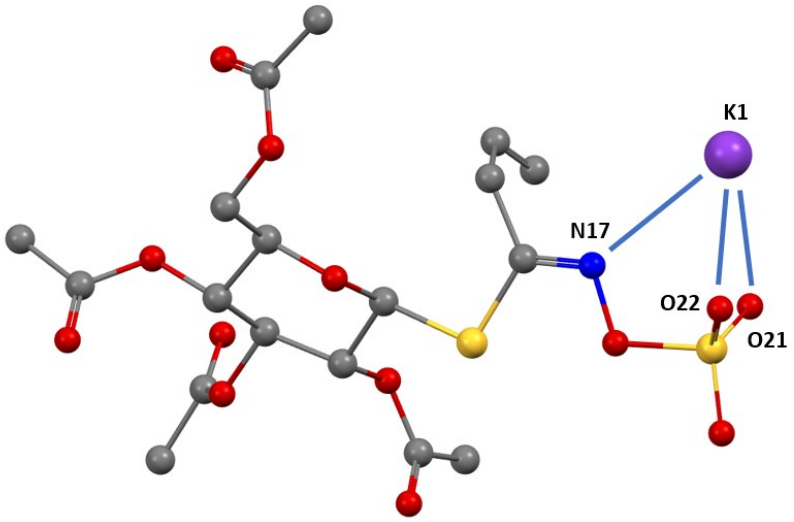

Fig. S8 DFT-optimized structure of K^+-**SinAc**$^-$ complex. Hydrogens are omitted for clarity.

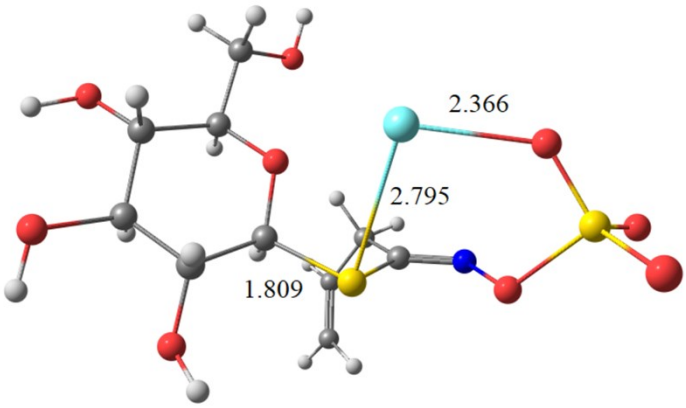

Fig. S9 DFT-optimized structure of Ag^{+}-**Sin**$^{-}$ complex based on structure **3c** (Fig. 3c).

	K·SinAc	**Ag·SinAc**
Empirical formula	$C_{18}H_{24}KNO_{13}S_2$	$C_{18}H_{21}AgNO_{13}S_2$
Formula weight	565.60	631.35
Temperature (K)	173	173
Wavelength (Å)	0.71073	0.71073
Crystal system	triclinic	monoclinic
Space group	*P*1	*C*2
Unit cell dimensions		
a (Å)	9.0195(2)	17.7902(8)
b (Å)	12.3261(4)	6.1119(2)
c (Å)	12.5871(3)	23.7144(10)
α (°)	101.321(2)	
β (°)	110.969(2)	110.671(5)
γ (°)	97.225(2)	
V (Å^3)	1251.57(6)	2412.51(18)
Z	2	4
Density(calcd) (g/cm^3)	1.501	1.738
Absorption coefficient (mm^{-1})	0.444	1.075
F(000)	588.00	1276.0
Crystal size (mm)	0.45 × 0.127 × 0.037	0.26 × 0.049 × 0.018
2*θ*max (°)	62	52
Index ranges *h*, *k*, *l*	-12…12, -17…17, -17…18	-21…21, -7…7, -29…29
Reflections collected	37676	13878
Independent reflections	12544	4763
Completeness	100.00	99.96
Transmission factors	0.707-1.000	0.611-1.000
Data/restraints/parameters	12544/3/639	4763/1/309
GOF on F^2	1.031	0.968
Final *R* indices [$I >= 2\sigma(I)$]	*R*1 = 0.0441, w*R*2 = 0.0993	*R*1 = 0.0445, w*R*2 = 0.0902
R indices (all data)	*R*1 = 0.0585, w*R*2 = 0.1049	*R*1 = 0.0750, w*R*2 = 0.0978
Largest diff peak and hole (e Å^{-3})	0.44/-0.38	0.79/-0.65
Flack parameter	-0.01(2)	0.00(2)

Table S1 Crystallographic and refinement parameters for **K·SinAc** and **Ag·SinAc**

Table S2 Selected bond distances of **K·SinAc**

Atom 1	Atom 2	Distance (Å)
C1	S12	1.800 (4)
C1B	S12B	1.802 (3)
S12	C13	1.747 (4)
S12B	C13B	1.761 (4)
N17	K35	2.987 (4)
N17B	K35B	2.943 (4)
O21	K35	2.813 (3)
O21B	K35B	2.775 (3)
O22	K35	2.912 (2)
O22B	K35B	2.870 (3)
O20	K35B	2.730 (2)
O20B	K35	2.606 (3)

Table S3 Selected bond distances of **Ag·SinAc**

Atom 1	Atom 2	Distance (Å)
C1	S12	1.803 (6)
S12	C13	1.736 (8)
C15	C16	1.34 (1)
C15	Ag1	2.465 (7)
C16	Ag1	2.332 (8)
N17	Ag1	2.412 (5)
O21	Ag1	2.365 (5)
O22	Ag1	2.519 (6)

Table S4 Selected bond distances for DFT-optimized structures of **SinAc**$^-$ compounds

Structure	Atom 1	Atom 2	Distance (Å)
SinAc$^-$	C1	S12	1.807
K^+-**SinAc**$^-$	C1	S12	1.808
	K1	N17	3.047
	K1	O21	2.872
	K1	O22	2.928
3a	C1	S12	1.810
	Ag1	N17	2.334
	Ag1	O22	2.498
3b	C1	S12	1.811
	Ag1	N17	2.594
	Ag1	O22	2.423
	Ag1	C15	2.728
	Ag1	C16	2.548
3c	C1	S12	1.812
	Ag1	S12	2.723
	Ag1	O22	2.420
	Ag1	O7	2.761
	Ag1	O33	2.443

Table S5 Cartesian coordinates, # of imaginary frequencies, and total energies of compounds **3a**, **3b**, and **3c**.

Compound **3a**			
O	1.35985100	-2.53189100	0.35666600
O	1.30067600	0.93927600	-0.71212200
O	4.72726600	0.78129600	0.48160300
O	0.99598900	-3.64956800	-1.57028500
O	4.10883500	-1.93951900	-0.18129500
O	6.04058200	0.73325400	-1.35541600
O	4.53695500	-2.51155300	1.96240100
C	0.79523900	-0.24178400	-0.13914500
H	0.61442200	-0.11442600	0.93745600
C	1.79538500	-1.38031100	-0.35343100
H	1.89087200	-1.61166300	-1.41898200
C	3.58379800	0.39281300	-0.27458600
H	3.84250100	0.34931900	-1.33683300
C	5.91285700	0.89726600	-0.16237400
C	2.46379700	1.40386600	-0.03910500
H	2.26222500	1.48527800	1.04030500
C	0.97047400	-3.61363700	-0.36013700
C	4.74187500	-2.65507100	0.77709600
C	3.14354900	-0.97480000	0.22444700
H	3.08745000	-0.96594100	1.31813100
C	0.50370900	-4.70505500	0.54553800
H	0.34523400	-5.61719800	-0.02780100
H	-0.43783100	-4.39884700	1.01253800
H	1.22979100	-4.87502500	1.34399500
C	7.00251200	1.24113400	0.80064700
H	6.72021000	2.11448600	1.39394600
H	7.92642600	1.43498000	0.25793100
H	7.14886500	0.40604000	1.49248400
C	5.70423400	-3.61862500	0.16150800
H	5.16427000	-4.31106200	-0.49056000
H	6.22345300	-4.17146100	0.94284700
H	6.42431800	-3.07736200	-0.45835100
O	1.72423500	3.63060600	-0.15314100
C	0.60691700	5.69082800	-0.08129200
H	-0.32676800	5.22111500	-0.40303500
H	0.66052100	6.71053100	-0.45984200
H	0.61104300	5.69982200	1.01236400
O	2.66638500	5.31844600	-1.29411200
C	1.77317200	4.90016100	-0.58543300
C	2.78106900	2.77176300	-0.58540200
H	2.82539300	2.75486500	-1.67839400
H	3.73619100	3.13137500	-0.19282000
S	-0.76497100	-0.68139500	-0.94430000
S	-4.55955900	-1.75656000	-0.68601800
O	-4.70641100	-2.67295400	-1.81482700
O	-3.40361700	-0.68330600	-1.33864800
O	-5.73555000	-0.89542200	-0.42097000
N	-3.12945400	0.35133000	-0.44150300
O	-3.92802500	-2.29414200	0.52337500
C	-1.87224400	0.45134400	-0.18952700
C	-1.43728000	1.52552400	0.75879900
H	-2.17868400	2.33322000	0.71693600
H	-0.49599600	1.96584200	0.41467900

C	-1.73991500	-0.13552200	2.64336800
H	-2.24081500	-0.86379700	2.00786000
H	-1.60805900	-0.39735100	3.68885700
C	-1.30444100	1.03728100	2.17912300
H	-0.81721600	1.74151500	2.85176200
Ag	-5.01180400	1.27413800	0.58348400

# of imaginary vibrational frequencies --- 0

PBE0 SCF energy --- -2673.09209295 A.U.

Compound **3b**

O	1.32346200	-2.55519100	0.30079200
O	1.31072400	0.92047000	-0.75368500
O	4.72094100	0.72684800	0.47921800
O	1.02050100	-3.68302900	-1.63089100
O	4.08380700	-1.98482800	-0.19664800
O	6.04983800	0.67186300	-1.34644300
O	4.47903300	-2.56514000	1.95111100
C	0.78178600	-0.26149500	-0.20764300
H	0.57008300	-0.14111400	0.86511700
C	1.77907400	-1.40642100	-0.40074100
H	1.89094300	-1.63773500	-1.46474400
C	3.58147700	0.35273400	-0.28927700
H	3.84898400	0.31308900	-1.34946500
C	5.91349100	0.83407400	-0.15424500
C	2.46722100	1.36967400	-0.05773900
H	2.25089500	1.44057700	1.01964500
C	0.97148500	-3.64665200	-0.42179100
C	4.69993700	-2.70658000	0.76850400
C	3.12214700	-1.01267300	0.19870300
H	3.05051900	-1.00708000	1.29153000
C	0.52355200	-4.75024500	0.47875100
H	0.30052800	-5.63858500	-0.11003400
H	-0.36978700	-4.43280000	1.02469500
H	1.30035600	-4.96933300	1.21611000
C	6.99748300	1.16636500	0.81900700
H	6.71778900	2.04135100	1.41113700
H	7.92781600	1.35278200	0.28472000
H	7.13017200	0.32885700	1.51066000
C	5.66574300	-3.67302400	0.16321500
H	5.13176400	-4.35947300	-0.50000600
H	6.17018300	-4.23207000	0.94978000
H	6.39797700	-3.13308900	-0.44345700
O	1.72939300	3.59412100	-0.15671400
C	0.56855500	5.63048100	-0.12026400
H	-0.35857700	5.10865900	-0.37255800
H	0.56946700	6.62686200	-0.55984000
H	0.61675800	5.70801700	0.96984900
O	2.62064900	5.27311500	-1.35060200
C	1.74520600	4.85328600	-0.62118900
C	2.79422900	2.74305800	-0.58456900
H	2.85379800	2.73812300	-1.67677400
H	3.74306800	3.09898700	-0.17374100
Ag	-4.31684900	0.44650600	1.60896600
S	-0.75433600	-0.67362300	-1.07343600
S	-5.14387300	-0.80952200	-1.45268700
O	-5.24261300	-2.04863000	-2.22125800
O	-3.45120500	-0.59297300	-1.48565600
O	-5.70635400	0.39417800	-2.06812100
N	-3.10681900	0.48336500	-0.68566300
O	-5.45519400	-0.95352200	-0.00795100
C	-1.85316400	0.52873600	-0.41740900
C	-1.46637600	1.61444700	0.55187100
H	-2.05673600	2.50287400	0.30343000
H	-0.42083800	1.91394600	0.42712900
C	-1.95582300	-0.01069000	2.45254100
H	-1.91062300	-0.89009400	1.81054900
H	-2.08720900	-0.18197900	3.51662800
C	-1.73796400	1.23592500	1.98427600
H	-1.70857700	2.06596800	2.68860300

# of imaginary vibrational frequencies --- 0

PBE0 SCF energy --- -2673.09440095 A.U.

Compound 3c

O	1.75496600	-2.56079000	0.19674000
O	0.39217800	0.80194900	0.37601800
O	3.92973300	1.64227600	0.43935000
O	1.07681000	-3.27246600	-1.83494800
O	3.89865000	-0.94268800	-0.76344700
O	4.41221400	2.47065400	-1.60586900
O	5.13068400	-1.76574500	0.94244400
C	0.46529800	-0.58259300	0.62645900
H	0.62052100	-0.79842600	1.69100200
C	1.59768700	-1.20428800	-0.19009400
H	1.38182700	-1.14201100	-1.26171200
C	2.74530300	1.02194000	-0.04969900
H	2.61633500	1.26362400	-1.10945100
C	4.70626600	2.32045100	-0.44103000
C	1.55342000	1.53179600	0.75808500
H	1.74121700	1.39289600	1.83296900
C	1.46220000	-3.52134400	-0.71476100
C	4.97570900	-1.57884600	-0.24397300
C	2.89570800	-0.47973800	0.13264800
H	3.20155100	-0.70505400	1.15963500
C	1.67584900	-4.87893200	-0.13170200
H	1.49404400	-5.63880300	-0.89002100
H	0.99237100	-5.02285400	0.71047700
H	2.69542000	-4.96373900	0.25348800
C	5.94070600	2.82809900	0.22951200
H	5.67883400	3.38233200	1.13423300
H	6.49744400	3.46429400	-0.45677700
H	6.56127300	1.97880300	0.53129000
C	5.91016600	-1.99972500	-1.33126900
H	5.40199100	-2.70082500	-1.99959900
H	6.79065000	-2.47176400	-0.89814600
H	6.20260200	-1.13077400	-1.92696200
O	0.14450800	3.41748300	1.25241500
C	-2.12670800	3.87257200	1.61695900
H	-2.18466200	3.15118500	2.43692800
H	-3.08272600	3.92115500	1.09812200
H	-1.88363600	4.84545400	2.05258900
O	-1.23029700	3.20450300	-0.51882200
C	-1.05499900	3.46179400	0.66255100
C	1.26100000	2.98852600	0.46803600
H	1.04758600	3.13548000	-0.59295300
H	2.10531100	3.60798600	0.77328000
Ag	-1.81296000	0.95701700	-1.27844300
S	-1.11204200	-1.29284800	0.08663100
S	-4.87344000	-0.56034800	-0.78026300

O	-4.97458700	-1.32799000	-2.02180400
O	-3.73709400	-1.51673200	0.04235700
O	-4.19592400	0.75510400	-0.90927500
N	-3.44258500	-0.99432600	1.31155500
O	-6.06764000	-0.51903500	0.06492300
C	-2.17661900	-0.87513400	1.45709600
C	-1.65564100	-0.39679900	2.77512700
H	-2.52188800	-0.03109900	3.33948800
H	-1.01469900	0.47865200	2.61309900
C	-0.83945100	-2.73003200	3.33310500
H	-1.31053400	-3.18308900	2.46388500
H	-0.29115100	-3.39332300	3.99490700
C	-0.92017200	-1.42433300	3.59214600
H	-0.43269200	-1.02113600	4.47845300

# of imaginary vibrational frequencies --- 0

PBE0 SCF energy --- -2673.09886099 A.U.

References

[1] Schultz, O.-E.; Wagner, W., *Arch*. *Pharm*., 1955, *288*, 525-532.

[2] Dolomanov, O. V.; Bourhis, L. J.; Gildea, R. J.; Howard, J. A. K.; Puschmann, H., *J. Appl. Crystallogr.* 2009, *42*, 339-341.

[3] Sheldrick, G. M., *Acta Crystallogr., Sect. A: Found. Crystallogr.* 2008, *64*, 112-122.

[4] Frisch, M. J.; Trucks, G. W.; Schlegel, H. B.; Scuseria, G. E.; Robb, M. A.; Cheeseman, J. R.; Scalmani, G.; Barone, V.; Petersson, G. A.; Nakatsuji, H.; Li, X.; Caricato, M.; Marenich, A. V.; Bloino, J.; Janesko, B. G.; Gomperts, R.; Mennucci, B.; Hratchian, H. P.; Ortiz, J. V.; Izmaylov, A. F.; Sonnenberg, J. L.; Williams-Young, D.; Ding, F.; Lipparini, F.; Egidi, F.; Goings, J.; Peng, B.; Petrone, A.; Henderson, T.; Ranasinghe, D.; Zakrzewski, V. G.; Gao, J.; Rega, N.; Zheng, G.; Liang, W.; Hada, M.; Ehara, M.; Toyota, K.; Fukuda, R.; Hasegawa, J.; Ishida, M.; Nakajima, T.; Honda, Y.; Kitao, O.; Nakai, H.; Vreven, T.; Throssell, K.; J. A. Montgomery, J.; Peralta, J. E.; Ogliaro, F.; Bearpark, M. J.; Heyd, J. J.; Brothers, E. N.; Kudin, K. N.; Staroverov, V. N.; Keith, T. A.; Kobayashi, R.; Normand, J.; Raghavachari, K.; Rendell, A. P.; Burant, J. C.; Iyengar, S. S.; Tomasi, J.; Cossi, M.; Millam, J. M.; Klene, M.; Adamo, C.; Cammi, R.; Ochterski, J. W.; Martin, R. L.; Morokuma, K.; Farkas, O.; Foresman, J. B.; Fox, D. J., Gaussian16. Gaussian, Inc.: Wallingford CT.

[5] Grimme, S.; Ehrlich, S.; Goerigk, L., *J. Comput. Chem.* 2011, *32*, 1456–1465.

[6] Grimme, S.; Antony, J.; Ehrlich, S.; Krieg, H., *J. Chem. Phys.* 2010, *132*, 154104.

[7] Tomasi, J.; Mennucci, B.; Cammi, R., *Chem. Rev.* 2005, *105*, 2999–3094.

[8] Glendening, E. D.; Landis, C. R.; Weinhold, F., *J. Comput. Chem.* 2013, *34*, 1429–1437.

[9] Zhurko, G. A.; Zhurko, D. A. *Chemcraft Version 1.8.* 2012.

[10] Miller, H. E.; The aglucone of sinigrin., *MA thesis*, Rice University, 1965.

[11] Pérez-Hernández, N.; Álvarez-Cisneros, C.; Cerda-Garcia-Rojas, C. M.; Morales-Rios, M. S.; Joseph-Nathan, P., *Magn*. *Reson*. *Chem*., 2013, *51*, 136-142.

[12] Waser, J.; Watson, W. H., Crystal structure of sinigrin. *Nature* 1963, *198*, 1297-1298.